Development of a Versatile Strategy for Inkjet-Printed Molecularly Imprinted Polymer Microarrays

Frank Bokeloh, Kasia Gibson, Karsten Haupt, Cédric Ayela

chemosensors

MDPI

Type of the Paper (Article, Review, Communication, etc.)

Development of a Versatile Strategy for Inkjet-printed Molecularly Imprinted Polymer Microarrays

Frank Bokeloh [1,2], Kasia Gibson [2], Karsten Haupt [1] and Cédric Ayela [2,*]

[1] Université de Technologie de Compiègne , CNRS Institute of Enzyme and Cell Engineering UMR7025, CS60319, 60203 Compiègne, France; e-mail: karsten.haupt@utc.fr
[2] Laboratoire IMS, Université de Bordeaux, CNRS, Bordeaux INP, UMR 5218, F-33607 Pessac, France; e-mail: cedric.ayela@ims-bordeaux.fr
* Correspondence: cedric.ayela@ims-bordeaux.fr; Tel.:+33540006540

Abstract: Biochips are composed of arrays of micropatterns enabling the optical detection of target analytes. Complementary to commercially available micro and nanospotters, ink-jet printing is a contactless and versatile micropatterning method. Surprisingly, the ink-jet printing of molecularly imprinted polymers (MIPs), also known as biomimetic synthetic antibodies, has not been demonstrated yet. In this work, core-shell structures are proposed, through the combination of ink-jet printing of the core (top-down approach) and controlled radical polymerization (CRP) to decorate the core by a thin film of MIP (bottom-up approach). The resulting biochips show quantitative, specific and selective detection of the antibiotic drug enrofloxacin by means of fluorescence analysis.

Keywords: Ink-jet printing; molecularly imprinted polymer; biochip

Citation: Lastname, F.; Lastname, F. Lastname, F. Title. *Chemosensors* **2022**, *10*, x. https://doi.org/10.3390/xxxxx

Academic Editor: Firstname Lastname

Received: date
Accepted: date
Published: date

1. Introduction

The integration of multiple lab processes on small chip-size substrates is one of the hot topics in the fields of biology and chemistry leading to the development of a large variety of lab-on-a-chip devices. The latter have the potential to replace heavy and complex laboratory equipment by miniaturized assays comprising low cost per chip, compactness, easy operational set-up, high speed, and reduced sample consumption [1,2]. Biochips are one simple and well-established example of lab-on-a-chip devices [3]. Classically, biochips are arrays of biomolecules immobilized on a small glass or silicon substrate [4]. They can be used for drug screening, environmental analysis and many other chemical or biological applications [5]. For these biochips, molecularly imprinted polymers (MIPs) offer an interesting alternative to the typically used biomolecules and were already reported in several applications [6,7]. MIPs in contrast to their natural counterparts are chemically and physically more stable, they can be chemically tuned, and shaped and processed on the micro- and nano-scale which makes them especially interesting for the integration as receptor element for lab-on-a-chip applications [8]. For this, various micro- and nanofabrication strategies for synthesis, patterning and processing MIPs have been developed over the past decades. While often based on light [9,10], mechanical methods, in particular micro-contact printing [11], mechanical spotting [12] and shadow-masking [13] have also been applied.

To fabricate biochips, mechanical deposition and patterning of small liquid volumes, are well-established approaches and commercially available nanospotters routinely deposit small patterns of droplets on a biochip [14]. However, the most popular mechanical spotting device is probably the inkjet printer, which reproduces digital images by precise, contactless deposition of small ink droplets on a substrate [15]. Until now, inkjet printers are widely spread and used not only by industry but also by private

consumers. Surprisingly, the inkjet-printing of MIPs has not been demonstrated yet. In this paper, the feasibility of inkjet-printed MIP microarrays is shown using an innovative strategy, which combines inkjet microprinting with a nanofabrication technique based on controlled radical polymerization (CRP). Key feature here is the use of an iniferter which enables the grafting of a thin MIP shell on top of the ink-jet printed core polymer by re-initiation and post-polymerization. As a target of the bioassays here we have chosen enrofloxacin, a quinolone antibiotic widely prescribed in veterinary medicine. This drug can, if used in excess, persist in the tissue of animals and therefore is a potential risk factor for consumers [16]. Thus analytical methods such as microbiological detection schemes are important to analyze and quantify quinolones [17]. Several articles have already demonstrated that MIPs offer an alternative approach of detecting these antibiotics [18-20]. In addition, enrofloxacin exhibits intrinsic fluorescence, which enables the evaluation of fabricated MIP patterns by epi-fluorescence microscopy [20].

2. Materials and Methods

2.1 Materials, Chemicals, Devices

All chemicals and solvents were of analytical grade and purchased from Sigma-Aldrich. PVDF Syringe filters with a pore size of 5 µm were obtained by Whatman. Microscope glass cover slips (15 mm x 15 mm) by Menzel were used as a substrate. The inkjet printer was a Jetlab 4 by Microfab equipped with a piezoelectrically actuated droplet generator and a Microfab glass microdispenser (aperture 50 µm). Patterned MIP features for binding evaluation were analyzed by an epi-fluorescence microscope equipped with a 10x/0.3 objective (Leica DM6000B). Pictures of other MIP patterns were taken by a fluorescence microscope equipped with a 2.5x/0.06 and 10x/0.06 objective. The thickness of single, inkjet-printed polymer drops was evaluated with an optical profilometer (Veeco 9080).

2.2 Design of Inkjet-Printed MIP Biochips

All presented polymer features were designed with Microsoft Paint and saved as a bitmap file. The three letters "MIP" were written in font style Calibri.

2.3 Sample and Substrate Preparation

2.3.1 Substrates

All samples were printed on microscopic cover glasses, surface modified with 3-(trimethoxysilyl)propyl methacrylate. For that, the glass slides were sonicated 15 minutes in a 2% solution of Hellmanex detergent, acetone, ethanol and isopropanol respectively. After drying the slides were activated by UV-ozone for 7 minutes and placed in a solution of 4 mmol 3-(trimethoxysilyl)propyl methacrylate in 200 ml ethanol and 6 ml of dilute acetic acid (1:10 glacial acetic acid:water). After ~10 minutes reaction time the samples were thoroughly rinsed with ethanol, isopropanol and dried. The method was adapted from the product information datasheet by Sigma-Aldrich [21].

2.3.2 Ink-jet Printing of Bulk MIPs

For the printing of bulk MIPs, 1 mmol enrofloxacin, 4 mmol methacrylic acid (MAA) and 4 mmol 2-hydroxethyl methacrylate (HEMA) were dissolved in 8.5 ml anhydrous butyronitrile. Next, 20 mmol of ethylene glycol dimethacrylate (EGDMA) and 0.24 mmol of Irgacure 819 polymerization initiator were added and the whole mixture purged with nitrogen for 5 minutes. Right before fabrication the mixture was transferred through a syringe filter to the sample cuvette of the inkjet printer. Samples were printed in the drop-on-demand mode by regulating the back-pressure between 8 - 12 mmHg and with a drop spacing of 211 µm for 71 pixels images. In a final step the inkjet-printed features

were transferred into a nitrogen pressured glove box and polymerized for 30 minutes using a 365 nm UV light source.

2.3.3 Ink-jet Printing of Core-shell MIPs

The core-shell MIPs were fabricated in two steps. For the printing process of the core polymer dots, 10 mmol trimethylpropane trimethacrylate (TRIM) and 1 mmol of benzyl-N,N-diethyldithiocarbamate (BDC) photoinitiator were dissolved in 2 ml o-xylene and filtered through a syringe filter prior to use. Samples were printed as described before but with varying drop spacing (211 µm for 71 pixels image; 180 µm for 101 pixels image; 148 µm for 101 pixels image; 130 µm for 101 pixels image). After fabrication samples were transferred to a nitrogen pressured glovebox and polymerized using a 312 nm UV light source (30 minutes). In a second step a MIP shell was grafted on top of the inkjet-printed core structure. For that, samples were transferred into a petri dish and covered with a MIP pre-cursor solution consisting of enrofloxacin (1.5 mmol), MAA (12 mmol), HEMA (12 mmol), EGDMA (60 mmol) and anhydrous acetonitrile (20 ml). The petri-dishes were placed under a 312 nm UV light source for polymerization (6 hours).

2.4 Evaluation of Fabricated Devices

Both bulk-MIP structures and core-shell structures were analyzed by fluorescence microscopy (Zeiss AX10). Bright field and fluorescence images were taken using a 2.5x / Na: 0.06 and a 10x / NA: 0.3 objective. Intrinsic fluorescence of enrofloxacin is used to evaluate the rebinding of the analyte into the MIP. The excitation/emission wavelengths were set at 280/440 nm for fluorescence measurements. Brightness and contrast were adjusted with the software ImageJ if necessary. The thickness of single, inkjet-printed polymer dots was evaluated with an optical profilometer (Veeco 9080).

2.5 Binding Tests of Core-Shell Structures

The binding properties of core-shell fabricated MIP assays were evaluated by equilibrium binding experiments. Before template extraction a fluorescence image of the structure was taken using a 10 x objective. The obtained fluorescence value was set to 1 as a reference point. After each extraction or binding step fluorescence images were taken. For template extraction the array was incubated 3 times 2h in acetic acid / ethanol (1:10) and rinsed thoroughly with acetonitrile. For binding studies the microarrays were exposed by 5 µM, 10µM, and 50 µM enrofloxacin in acetonitrile for at least 2 hours. Extraction and incubation times may be optimized for a given MIP composition and layer thickness. To assess the specificity of the MIP, the same structure was exposed to 50 µM enrofloxacin and after extraction to 50 µM flumequine. The fluorescence intensity was analyzed with the software ImageJ. The region of interest was selected and the values "area" and "integrated density" were measured. Next, the non-fluorescent background was analyzed by measuring the "mean grey value". The corrected fluorescence was calculated by [22]:

$$Fluorescence_{Corr;Norm} = integrated\ Density - (area \times mean\ gray\ value)$$

3. Results

For initial tests, non-imprinted polymer features based on TRIM were inkjet-printed printed on a 15 x 15 mm² microscope cover glass. For that, two regions were defined on the glass: For the evaluation of binding properties and the characterization of the droplet size, a pattern of single droplets was printed on one side of the substrate. To prove the feasibility of printing complex structures on a micron scale, the three letters "MIP" were printed on the other half of the microarray chip. A schematic illustration of the microarray chip and two microscope images of the two areas is presented in Figure 1. One of the

big advantages of inkjet-printing is that it is based on direct writing and no additional masks, as used for standard photolithography, or stamps for soft-lithography are needed. Thus, different designs could be simply generated and modified with the Paint software of Microsoft.

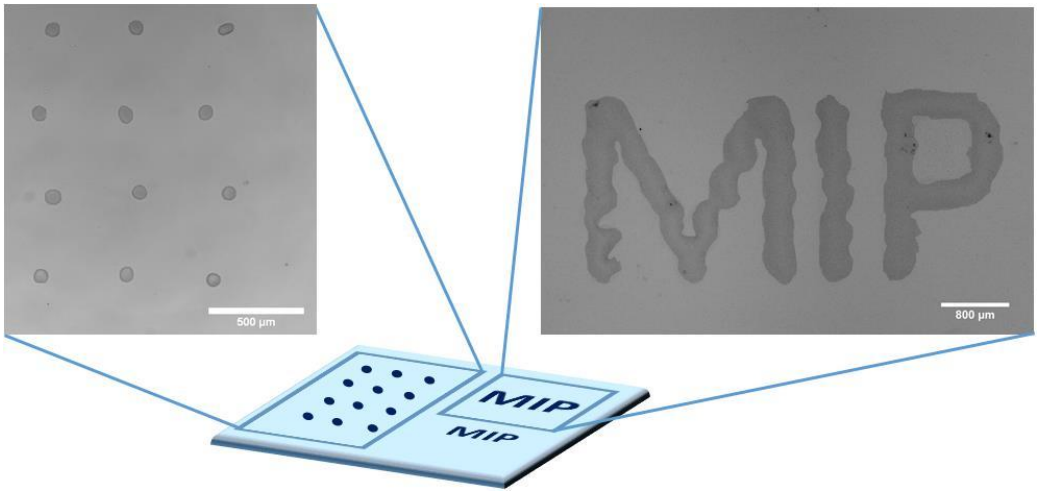

Figure 1. Design of the inkjet-printed MIP microarray with microscopic images of a pattern of 12 droplets, in a zig-zag shape (left), and the inkjet-printed letters "MIP" (right), both based on TRIM.

For many microfabrication methods of MIPs (and polymers in general), the viscosity of formulation has to be adjusted and formulations with higher density have to be used to create well-defined polymer patterns. The adjustment of the viscosity is also for inkjet printing one important parameter. If the viscosity is too low, printed droplets will spread more easily, whereas too viscous inks are difficult to process. Typical ink formulations for inkjet applications have a viscosity of 2 cP [23], although for special applications printer systems have been reported that can handle highly viscous inks between 20 and 100000 cP [24]. The viscosity of the samples in our experiments were adjusted to 5 cP by adding 50 wt% o-xylene to the TRIM monomer. Separated and homogeneous polymer droplets were printable with formulated pre-polymer mixtures and the viscosity was low enough to allow the channel of the ink jet nozzle to be refilled in 100 µs (Figure 1). Next to the viscosity the surface tension of the substrate and the hydrophobicity of the ink are crucial parameters for inkjet-printed features. Therefore, extensive cleaning of the substrate was essential in order to obtain homogeneous printed patterns. The hydrophobic solvent o-xylene was chosen for the viscosity adjustment of TRIM and enabled to print uniform droplets that did not spread on the surface of the substrate. Furthermore, the solvent o-xylene is less volatile than the more commonly used toluene and thus does not evaporate too quickly. High evaporation rates of the solvent could result in a volume change of printed droplets and heterogeneous print pattern or even block the nozzle of the printer before printing. This is especially important for small volumes such as inkjet-printed droplets (volume in the picoliter range), that are more effected by evaporation, due to their larger surface to volume ratio. Concretely, feature sizes of 65µm in diameter and 6.7µm in thickness were determined with an optical profilometer (Figure 2d). The drop spacing was the main value which was varied in order to obtain homogeneously patterned structures. Figure 2a-c presents three polymer patterns with a drop spacing of 211µm (image size 71 pixel); 200µm (image size 101 pixel) and 180µm (image size 101 pixel) respectively. It can be seen that by adjusting the drop spacing individual printed droplets merge and a homogeneous pattern can be achieved (Figure 2c). Figure 2b shows a half-merged structure. This might be the result of a heterogeneous surface tension and mechanical movements of the drops. According to the requirements of the application the print settings can be adjusted to print separated small droplets or bigger

feature sizes. For most inkjet applications, the drop spacing is set to a value that the ink on the substrate merges with each other.

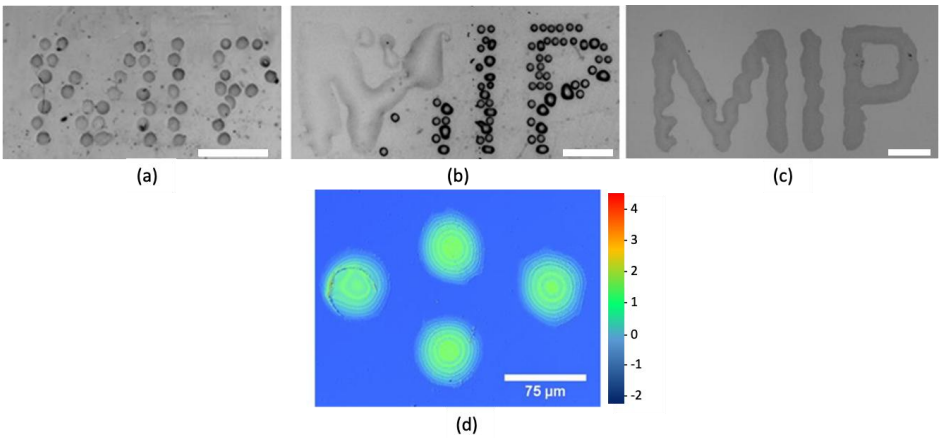

Figure 2. (a)-(c) Brightfield images of polymerized "MIP" pattern inkjet printed with different droplet spacing results in separated droplets, half merged droplets and total merged droplets. Scale bar is 800µm; (d) Optical profilometer image of separated inkjet-printed polymer droplets.

We then moved to the fabrication of MIP structures. Two concepts for the fabrication of inkjet-printed microarrays based on MIPs have been investigated. Figure 3 illustrates the two approaches that were employed for the development of MIP arrays targeting the drug enrofloxacin. In a first approach (A) a MIP precursor was directly printed on the substrate and polymerized with a 365 nm UV light source. Mechanical deposition for the direct microfabrication of a microarray based on MIPs was already proposed by writing MIP microstructures with a nanofountain pen [12] or with a silicon cantilever matrix [25]. However, the direct writing of MIPs by inkjet printing has never been demonstrated. In a second approach (B) a core polymer pattern was printed from the trifunctional cross-linking monomer TRIM in a first step. The key feature of this approach was the use of the iniferter-type polymerization initiator BDC. This CRP initiator creates under UV irradiation one radical that initiates polymerization and one "stable" radical, capable of terminating the growing polymer chain by recombination [26]. As a consequence, these molecules exhibited a 'living' character of the polymerized TRIM core and a second polymer layer, the MIP shell, can be grafted on top through post-polymerization after re-initiation. The combination of microfabrication methods and iniferter-based polymerization was already proposed in a more chemical approach, where the iniferter was covalently bond to a silicon bead, suggesting that this approach could be transferred to microfabrication techniques such as photolithography. The advantage of this technique is the versatility. The polymer core can be fabricated from different materials of different viscosity and thus can be potentially adapted by many other microfabrication techniques, such as photolithography or soft-lithography [27]. Once optimized for a given application, however, it does not need re-adaption with respect to a specific MIP. Indeed, this technique allows for the integration of many MIPs already described in the literature without changing the established ink-jet printing formulation and conditions.

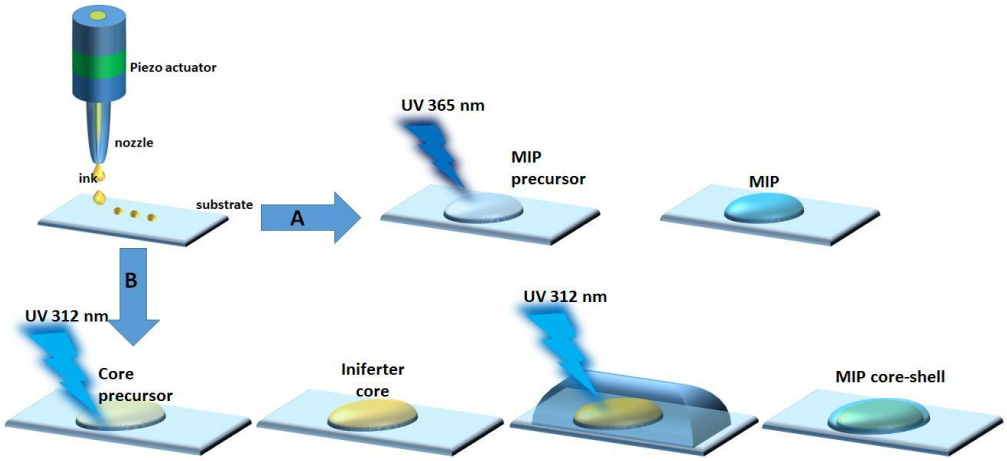

Figure 3. Two concepts of inkjet printed MIP arrays. A) direct patterning of MIP formulation; B) Core-shell approach: a core made of TRIM is patterned and polymerized with the iniferter BDC. A shell made of MIP is grafted in a second step by reinitiating the polymerization.

For the direct approach the MIP targeting enrofloxacin was printed directly on the substrate. Butyronitrile was used as a porogenic solvent of the MIP precursor solution. This solvent was used by Barrios and co-worker to fabricate a MIP diffraction grating targeting enrofloxacin [28]. Butyronitrile is less volatile than the commonly used acetonitrile and should be less prone to evaporation. In Figure 4a and b the "MIP" pattern and a droplet of printed and polymerized MIP solution is presented. Since butyronitrile is in contrast to xylene a polar solvent, printed features spread on the surface of the substrate, leading to a reduced resolution of the printed pattern. The droplets spread in non-uniform directions and had feature sizes between 500 µm and 800 µm. Although the less volatile solvent butyronitrile was used for fabrication, the solvent evaporated too quickly from the very thin printed layer and as a consequence the template molecule enrofloxacin precipitated in thin needles within the polymer structures. One possibility of overcoming these issues was replacing the solvent butyronitrile. The hydrophobic solvent 1-methylnaphthalene was able to dissolve enrofloxacin, and structures with smaller feature size and uniform spread could be fabricated (Figure 4c). Also in some patterned drops the template precipitated, some droplets polymerized as a homogenous polymer with the template dissolved in the polymer matrix. However, changing the MIP formulation from a polar solvent such as acetonitrile or butyronitrile towards a nonpolar solvent can interfere with the binding properties. Furthermore, it turned out that the evaluation of the binding was challenging due to the big fluorescence background of the bulk polymer. Thus, we changed our strategy and instead of a bulk polymer pattern decided to rely on a core-shell structure.

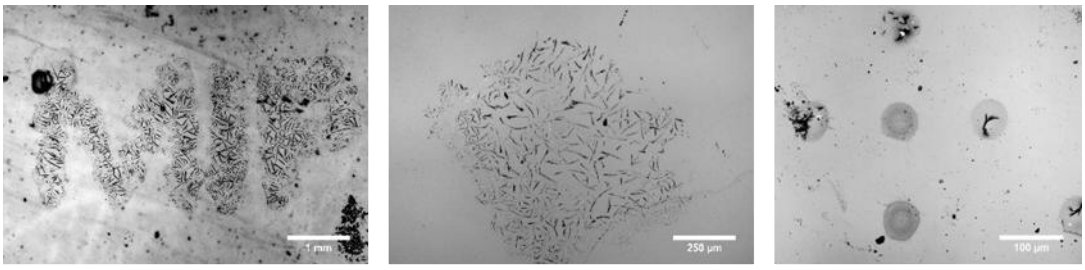

(a) (b) (c)

Figure 4. (a), (b) Brightfield images of MIP pattern and polymerized droplet of a MIP with the solvent butyronitrile. Enrofloxacin precipitates as little needles; (c) Polymerized droplets using 1-methlynaphthalene as solvent.

The size and heights of printed iniferter-polymer cores are shown on Figure 2. After polymerizing the core polymer, a thin MIP layer was polymerized by re-initiation with the iniferter BDC. Due to the dimensions (50 to 60 µm) and the spherical shape of the core, it was difficult to analyze the thickness of the shell, which was estimated to be in the nanometer range. Sellergren and co-workers reported shell thicknesses of around 15 nm [27], whereas Marchyk and co-workers found shell thicknesses, depending on the fabrication conditions, between 5 nm and 116 nm [29]. Since similar conditions were used to graft the MIP shell, it can be assumed that in our case the shell thickness was between 10 nm and 100 nm. The success of the MIP-shell grafting could be verified by fluorescence microscopy due to the template enrofloxacin in the MIP. Indeed, a bright fluorescence was observed after the grafting step (Figure 5c). The living character of the core-bound BDC was demonstrated by a control experiment using the conventional FRP initiator Irgacure 819 instead of the iniferter, resulting in no significant increase in fluorescence.

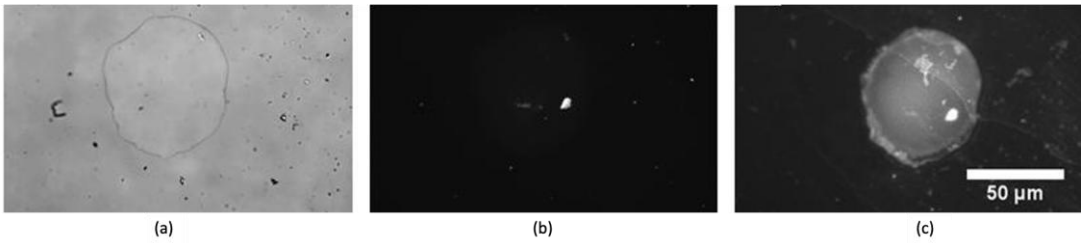

Figure 5. (a) Brightfield image of iniferter-polymerized core; (b) Corresponding fluorescence image after core fabrication; (c) Resulting fluorescence image after MIP grafting.

The binding properties of fabricated core-shell structures were analyzed by epifluorescence microscopy. The fluorescence value obtained after fabrication was normalized and used as reference point. After extraction of the template molecule with acetic acid / ethanol (1:10) (three rounds, 2 hours each) the polymer structure was thoroughly rinsed with acetonitrile and dried. The fluorescence intensity after extraction decreased by approximately 60 % of the initial value (Figure 6a and 6c). Remaining fluorescence was attributed to the template which was trapped in the polymer matrix and could not be extracted from the polymer. Figure 6a shows a MIP-grafted ink-jet printed polymer structure after fabrication, after template extraction and after incubation in 50 µM of enrofloxacin, respectively. The increase in fluorescence proofs the uptake of the analyte into the binding sites. After incubation for 2 hours in 5 µM, 10 µM and 50 µM of enrofloxacin in acetonitrile solutions, fluorescence images were taken and analyzed. The increasing fluorescence intensity showed a dependence on the analyte concentration (Figure 6b). Binding specificity of the fabricated MIP was evaluated using a chemically identical control non-imprinted polymer (NIP), and by incubating the structures in 50 µM flumequine as a structural analogue (Figure 6a). The fluorescence increase was significantly less for flumequine than for enrofloxacin, indicating that the MIP specifically targets enrofloxacin. Also, a low fluorescence signal was measured on NIP control after incubation in 50µM enrofloxacin, showing again the specific detection of analyte by the patterned MIP. These results are in good agreement with earlier reports on MIPs targeting enrofloxacin [16, 30].

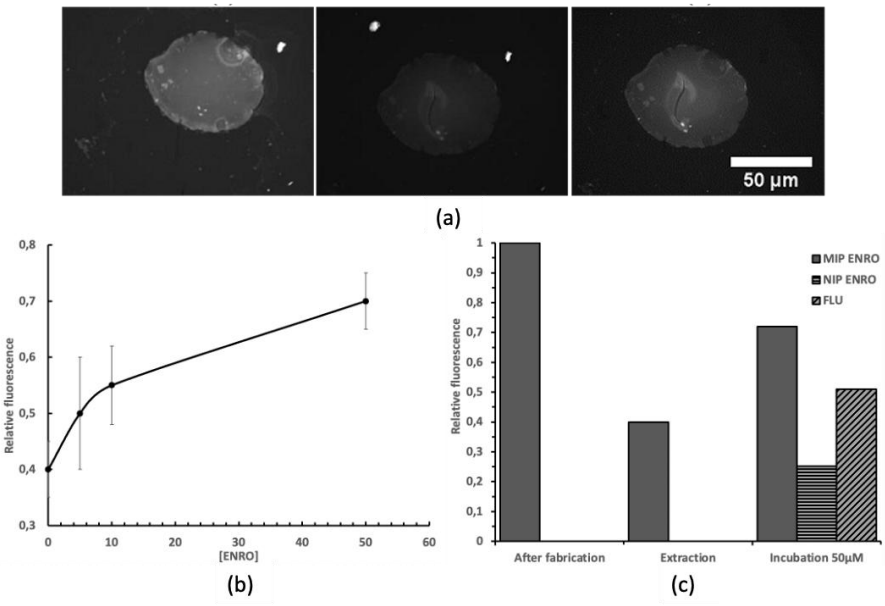

Figure 6. (a) Enrofloxacin imprinted structure after fabrication; after extraction and after binding 50 µM enrofloxacin; (b) Binding results with 5 µM, 10 µM and 50 µM enrofloxacin; number of experiments n=3, error bars represent the standard error of the mean; (c) Specificity and selectivity studies with 50 µM enrofloxacin on both MIP and NIP vs 50 µM flumequine.

4. Conclusions

In this paper, a microfabrication strategy for microarrays based on MIPs was presented. By inkjet printing of a TRIM-based prepolymer mixture containing an iniferter as a living polymerization initiator, a polymer pattern was generated on a substrate, onto which a MIP shell targeting enrofloxacin was subsequently grafted by re-initiation and post-polymerization. Thus, a microfabrication (top down) and a nanofabrication (bottom-up) approach were merged with each other. The obtained MIP shells were analyzed by fluorescence microscopy and binding characteristics of the MIP shell were found in agreement with the literature, proofing specific target binding and thus the success of the method. One of the advantages of the described method is its versatility. To produce biochips composed of arrays of several different (multiplexed) MIPs, both top-down and bottom-up approaches are suitable. Thus, the inkjet writing can be easily combined with localized photopolymerization (e.g. by projection photolithography), or by localized deposition of the MIP precursors (e.g. approaches similar to soft-lithograph). Also the grafted MIP can be directly adapted from the huge library of already existing MIPs [31] and is therefore not limited by adjustments that have to be made for microfabrication.

Author Contributions: Conceptualization, F.B. and C.A.; methodology, F.B., K.B. and K.H.; investigation, F.B. and K.B.; writing—original draft preparation, F.B. and C.A.; writing—review and editing, C.A. and K.H.; supervision, C.A. and K.H.; funding acquisition, K.H. All authors have read and agreed to the published version of the manuscript.

Funding: This research was funded by the European Union Marie Curie Actions (grant number FP7-PEOPLE-2013-ITN-607590, SAMOSS project).

Data Availability Statement: Not applicable.

Acknowledgments: The authors would like to acknowledge ElorprintTec, a clean-room facility at the University of Bordeaux for technical support.

Conflicts of Interest: The authors declare no conflict of interest.

References

1. Persidis A. *Nat Biotech* **1998**, 16, 981–983.
2. Kamar, A.Z. ; Shamzi, M.H. *Micromachines* **2020**, 11(2), 126.
3. Fruncillo, S. ; Su, X. ; Liu, H ; Wong, L.S. *ACS Sens.* **2021**, 6, 2002.
4. Park, M. ; Kang, B-H.; Jeong, K-H. *BioChip J.* **2018**, 12, 1.
5. Azizipour, N.; Avazpour, R., Rosenzweig, D.H. ; Sawan, M. ; Ajji, A. *Micromachines* **2020**, 11, 599.
6. London, J.W.; Diliën, H.; Singla, P.; Peeters, M.; Cleij, T.J.; Van Grinsven, B.; Eersels, K. *Sens. Actuators B* **2020**, 325, 128973.
7. Refaat, D. ; Aggour, M.G. ; Farghali, A.A.; Mahajan, R.; Wiklander, J.G.; Nicholls, I.A.; Piletsky, S.A. *Int. J. Mol. Sci.* **2019**, 20, 6304.
8. Bokeloh, F.; Ayela, C.; Haupt, K. Micro and Nanofabrication Methods of Molecularly Imprinted Polymers. In *Molecularly Imprinted Polymers for Analytical Chemistry Application*, Chapter 6, Royal Society of Chemistry, 2018.
9. Haupt, K.; Linares, A.V; Bompart, M. *Top. Curr. Chem.* **2012**, 325, 1–28.
10. Paruli, E. III.; Soppera, O.; Haupt, K.; Gonzato, C. *ACS Appl. Polym. Mater.* **2021**, 3, 4769–4790.
11. Lalo, H.; Ayela, C.; Dague, E.; Vieu, C.; Haupt, K. *Lab Chip* **2010**, 10, 1316.
12. Belmont, A-S.; Sokuler, M.; Haupt, K.; Gheber, L.A. *Appl. Phys. Lett.* **2007**, 90, 193101.
13. Ayela, C.; Dubourg, G.; Pellet, C.; Haupt, K. *Adv. Mater.* **2014**, 26(33), 5876-5879.
14. Arrabito, G.; Gulli, D.; Alfano, C.; Pignataro, B. *Analyst* **2022**, 147, 1294.
15. Li, X.; Liu, B.; Pei, B. ; Chen, J. ; Zhou, D. ; Peng, J. ; Zhang, X. ; Jia, W. ; Xu, T. *Chem. Rev.* **2020**, 120, 10793**.**
16. Caro, E.; Marcé, R.M.; Cormack, P.A.G.; Sherrington, D.C.; Borrull, F. *Anal. Chim. Acta* **2006**, 562, 145–151.
17. Okerman, L.; Noppe, H.; Cornet, V.; De Zutter, L. *Food Addit. Contam.* **2007**, 24, 252–257
18. Wang, D.; Jiang, S.; Liang, Y.; Wang, X.; Zhuang, X.; Tian, C.; Luan, F.; Chen, L. *Talanta* **2022**, 236, 122385.
19. Wang, W.; Wang, R.; Liao, M.; Kidd, M.T. *Food Measure.* **2021**, 15, 3376-3386.
20. Liu, X.; Ren, J.; Su, L.; Gao, X.; Tang, Y. ; Ma, T. ; Zhu, L. ; Li, J. *Biosens. Bioelectron.* **2017**, 87, 203-208.
21. Sigma-Aldrich. Available online: www.sigmaaldrich.com/content/dam/sigma-aldrich/docs/Sigma/Product_Information_Sheet/1/m6514pis.pdf .
22. McCloy, R.A.; Rogers, S.; Caldon, C.E.; Lorca, T.; Castro, A.; Burgess, A. *Cell Cycle* **2014**, 13, 1400–1412.
23. Calvert, P. *Chem. Mater.* **2001**, 13, 3299–3305.
24. Yang, H.; He, Y.; Tuck, C.; Wildman, R.; Ashcroft, I.; Dickens, P.; Hague, R. in Proceedings of 24th Annual International Solid Freeform Fabrication Symposium: An Additive Manufacturing Conference, Austin, TX, USA, 2013.
25. Vandevelde, F.; Leïchlé, T.; Ayela, C.; Bergaud, C.; Nicu, L.; Haupt, K. *Langmuir* **2007**, 23, 6490.
26. Beyazit, S.; Tse Sum Bui, B.; Haupt, K.; Gonzato, C. *Prog. Polym. Sci.* **2016**, 62, 1.
27. Sellergren, B.; Rückert, B.; Hall, A.J. *Adv. Mater.* **2002**, 14, 1204– 120
28. Barrios, C.A.; Zhenhe, C.; Navarro-Villoslada, F.; López-Romero, D.; Moreno-Bondi, M.C. *Biosens. Bioelectron.* **2011**, 26, 2801.
29. Marchyk, N.; Maximilien, J.; Beyazit, S.; Haupt, K., Tse Sum Bui, B. *Nanoscale* **2014**, 6, 2872.
30. Ton, X-A; Acha, V.; Haupt, K.; Tse Sum Bui, B. *Biosens. Bioelectron.* **2012**, 36, 22–28.
31. mipdatabase. Available online: www.mipdatabase.com